



**HAL**  
open science

## Acoustic source localization based on the similarity rate between frequency-time images

Karl Hourany, Youssef Zaatar, Farouk Benmeddour, Emmanuel Moulin,  
Dorothee Debavelaere-Callens, Jamal Assaad

### ► To cite this version:

Karl Hourany, Youssef Zaatar, Farouk Benmeddour, Emmanuel Moulin, Dorothee Debavelaere-Callens, et al.. Acoustic source localization based on the similarity rate between frequency-time images. 1st International Conference on Sensors, Networks, Smart and Emerging Technologies (SENSET 2017), Sep 2017, Beriut, Lebanon. 10.1109/SENSET.2017.8125008 . hal-03280235

**HAL Id: hal-03280235**

**<https://uphf.hal.science/hal-03280235>**

Submitted on 11 Jul 2022

**HAL** is a multi-disciplinary open access archive for the deposit and dissemination of scientific research documents, whether they are published or not. The documents may come from teaching and research institutions in France or abroad, or from public or private research centers.

L'archive ouverte pluridisciplinaire **HAL**, est destinée au dépôt et à la diffusion de documents scientifiques de niveau recherche, publiés ou non, émanant des établissements d'enseignement et de recherche français ou étrangers, des laboratoires publics ou privés.



Distributed under a Creative Commons Attribution 4.0 International License

# Acoustic source localization based on the similarity rate between frequency-time images

K. Hourany and Y. Zaatar

Applied Physics Laboratory, Faculty of Sciences  
Lebanese University, PoB 90656 Jdeidet  
Fanar, Lebanon

F. Benmeddour, E. Moulin, D. Callens, and  
J. Assaad

IEMN UMR CNRS 8520, Université de  
Valenciennes et du Hainaut-Cambrésis, F59313  
Valenciennes cedex 9, France

**Abstract** — Many studies in different domains have shown the possibility of extracting information from a medium by exploiting the natural acoustic noise present in such medium. Recently, the promising potential of a passive acoustic technique, based on the correlation of the ambient noise for controlling the state of the structures has been shown. The position of the acoustic source should be determined at the time of the measurement. In this study we will apply an algorithm explained in a previous work in order to locate an unknown source position based on the calculation of the similarity rate between frequency-time images related to the ambient noise correlation.

**Keywords** — *structural health monitoring; frequency-time images; correlation; acoustic source; similarity rate*

## I. INTRODUCTION

In many domains such as the underwater acoustics [1-3] and seismology [4-6], several studies have been conducted and they have shown that it is possible to extract information related to a medium by exploiting the natural acoustic noise in this medium, this allows a passive detection method. Recent studies have shown the promising potential of such a technique based on the correlation of an acoustic field [7]. The advantage of this technique is that it allows an on-site and real time control.

In the theoretical case of a perfectly diffuse field, the correlation function depends on the properties of the structure and the presence of a defect in this structure. Otherwise, the correlation function depends also on the characteristics of the source (its position for example) which may vary from one measurement to another. Among some of the works that have used the assumption of a non-diffuse field [8] it may be mentioned the work of Abou Leyla *et al.* [9-11] which proposes the use of a sensor called reference sensor in order to identify the configuration of the source at the time of measurement.

The system consists of a pair of acoustic receivers. The principle being to build a database containing the frequency-time images of the cross-correlations of the

signals received on two measurement sensors (A and B) for the healthy state of the structure.

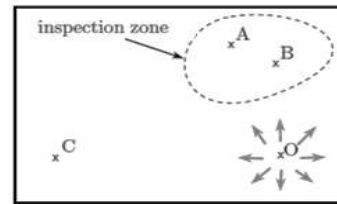


Fig. 1. Descriptive schematic of the problem (O represents a source).

This database should also contain the frequency-time images of the autocorrelations of the signals received on the reference sensor (C) for the possible source configurations. Then at each measurement, the frequency-time image of the cross-correlation is compared to its reference for the identified source configuration. Henceforth, these frequency-time images will be simply named images.

In this work, the comparison of these images will be made automatically using a method based on the local minima present in these images. The calculation of the degree of resemblance between these images leads us to locate an unknown source position.

## II. SIMULATION OF A REVERBERANT PLATE

Consider a rectangular plate having a length of 1 m and a width of 0.5 m, an emitter S and a receiver R having the positions indicated in figure 2.

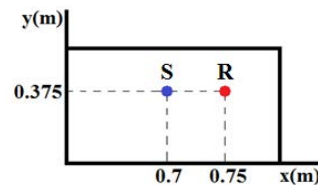


Fig. 2. Positions of the emitter S and the receiver R.

The excitation signal  $S_{f_0}(t)$  is a sinusoidal pulse of 5 cycles of sinusoids and having a center frequency  $f_0$  varying from 8 kHz to 15 kHz with a step of 5 Hz. This sinusoidal pulse is written as follows:

$$s_{f_0}(t) = w(t) \sin(2\pi f_0 t). \quad (1.1)$$

In the previous equation,  $w(t)$  represents the Hanning window:

$$w(t) = \begin{cases} \frac{1 - \cos\left(\frac{2\pi f_0 t}{N_c}\right)}{2} & 0 \leq t \leq T, \\ 0 & t > T \end{cases} \quad (1.2)$$

where  $N_c$  is the number of the sinusoidal cycles and  $T = N_c T_0 = N_c / f_0$  is the duration of the window.

An example of the excitation signal  $f_0 = 8$  kHz is shown in figure 3.

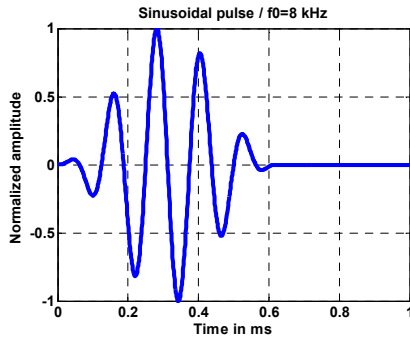


Fig. 3. Sinusoidal pulse with a center frequency  $f_0 = 8$  kHz.

The signal received at the receiver R, after reflections on the edges of the plate, is calculated using the source image method which is mainly used in room acoustics [12, 13]. In fact, a reflected signal received at the receiver for any position, is seen as a direct wave from a virtual image source. In our case, the structure has four reflection plans; thus the original source has four virtual source images, each image with respect to one of these plans. So in the first order, the receiver R receives five waves (a direct one from S to R and four reflected on the four edges of the plate). The second order will be the images of the source images in the first order with respect to the plans and so on.

The signal received at the receiver R is simulated using an order of reflection equal to 40 and it is represented in figure 4.

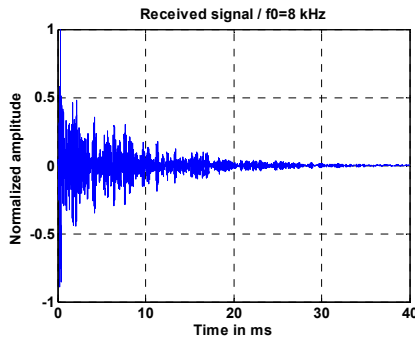


Fig. 4. Signal received at the receiver R.

Finally, rather than working on rough correlations, a frequency-time representation is more appropriate for highlighting the interesting effects. Note that the choice of working with the envelope of the autocorrelation and not with the autocorrelation itself has been made, because with the envelope the number of local minima will be reduced in the image as these local minima represent the minima in the autocorrelation signal. The previous simulation is repeated for frequencies  $f_0$  which vary from 8 kHz to 15 kHz to finally obtain the image of the envelopes of the autocorrelation of the signals received at the receiver R when the emitter S is emitting a sinusoidal pulse of 5 cycles of sinusoid.

Figure 5 shows a part of the image for the positions of the emitter S and the receiver R represented in figure 2. Note that the image is limited to 2 ms in order to better visualize the local minima in this image (they are none other than the dark areas). The area circled in figure 5 represents one local minimum of this image.

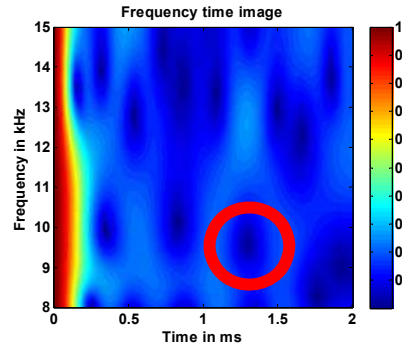


Fig. 5. Frequency-time image.

By applying the comparison algorithm explained in a previous work [14], these local minima can be extracted (represented by dots in figure 6).

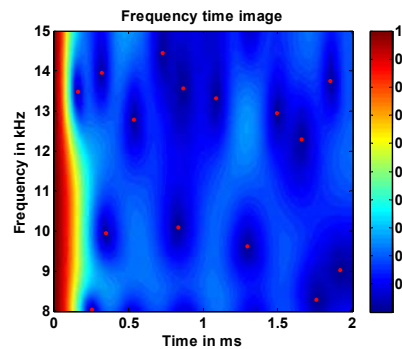


Fig. 6. Frequency-time image and the extracted local minima.

In this section, we explained the simulation of the propagation of a signal in a rectangular plate as well as the extraction of the corresponding autocorrelation image. The simulation results were given for a fixed position of the emitter and the receiver. In the next section, the source position will be considered as unknown then it will be shown how we can locate it.

### III. LOCALIZATION OF AN UNKNOWN SOURCE

Consider the positions of the source and the receiver shown in the figure 7 as follows:

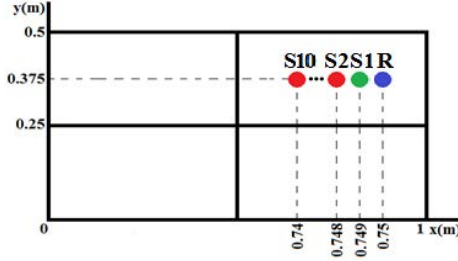


Fig. 7. Positions of the source and the receiver.

The receiver is set at a position having (0.75 cm, 0.375 cm) as coordinates and the source moves from the position  $S_1$  (0.749 cm, 0.375 cm) to the position  $S_{10}$  (0.74 cm, 0.375 cm) with a step of 1 mm. The image of the position  $S_1$  is considered as the reference image and it will be compared to the images of the other positions ( $S_1$ - $S_{10}$ ), so the similarity rate between the images  $S_1$  and  $S_1$ ,  $S_1$  and  $S_2$  throughout  $S_{10}$ , will be calculated.

Similarly, the images are extracted for each position of the source  $S$  and the algorithm is applied to extract the local minima in order to subsequently calculate the similarity rate. The variation of the average of distances depending on the positions of the source is represented in figure 8.

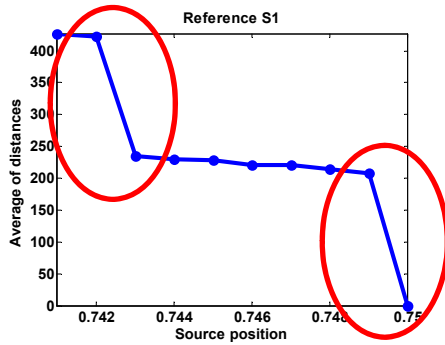


Fig. 8. Average of distances depending upon the positions of the source.

In order to deal with the similarity rate instead of the average of distances, the following equation will be applied:

$$\text{similarity rate} = 100\% \left( \frac{\text{average of distances obtained}}{\text{maximum average of distances}} \right) \% \quad (1.3)$$

where the maximum average of distances is non-other than the Euclidian distance of the diagonal of the image.

The variation obtained in figure 8 is not linear due to the jumps existing between the positions  $S_1$  and  $S_2$ , and between the positions  $S_8$  and  $S_9$  (circled area), which are caused by the disappearance of a local minimum in the

transition from  $S_1$  to  $S_2$  and  $S_8$  to  $S_9$  as shown in the figure 9.

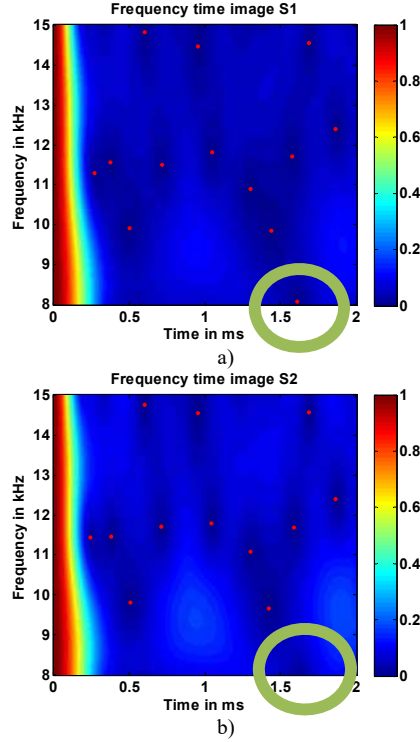


Fig. 9. Representation of the disappearance and the local minimum at the passage from a)  $S_1$  to b)  $S_2$ .

In order to get a linear variation, a weighting process by the Hanning window in time and frequency is used to reduce the effect of the local minima at the edges of each image. The process of weighting is made according to the following steps.

First, the corresponding local minima of the positions  $S_1$  and  $S_2$  are plotted as shown in figure 10.

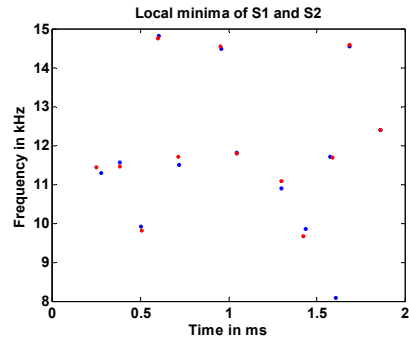


Fig. 10. Local minima of  $S_1$  and  $S_2$ .

Then the midpoint is sought between a minimum of the image corresponding to  $S_1$  and its nearest neighbor in the image corresponding to  $S_2$ . When a point does not have a neighbor, then it is considered itself a midpoint.

After determining the midpoints, each distance (between a minimum and its neighbor) is multiplied by

the value  $\alpha$  (corresponding to the Hanning window in time) and the value  $\beta$  (corresponding to the Hanning window in frequency) as shown in figure 11. These values correspond to the midpoint relative to this distance. The average of all the weighted distances allows obtaining the weighted average between the images of  $S_1$  and  $S_2$ .

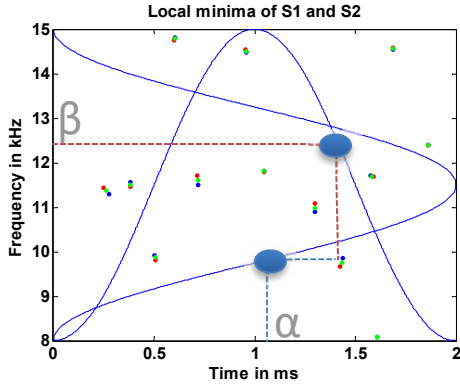


Fig. 11. Example of the weighting process

Finally, after applying this process for all the positions ( $S_1$ - $S_{10}$ ), the weighted average of the distances is plotted as a function of the position of the source  $S$ . Figure 12 shows a comparison between the cases with and without weighting. Both curves have been normalized so that they will be compared on the same scale.

After weighting, the jumps disappeared and the variation has become almost linear. Therefore an unknown source position can be localized after calculating the average of the distances between the local minima of an image relative to the unknown position and that of the reference position.

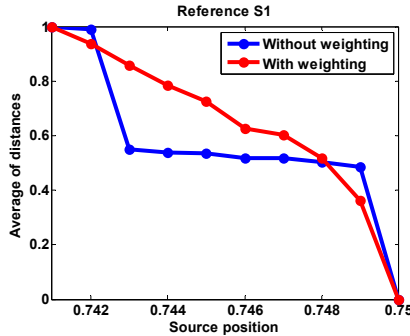


Fig. 12. Comparison between with and without windowing

#### IV. CONCLUSION

This paper illustrates the simulation results on the application of a comparison algorithm explained in a previous work. First, the mode to simulate the propagation of a signal has been explained. Then the algorithm is applied in order to compare frequency-time images. The jumps present in figure 8; representing the variation of the average distance as a function of the

source position, due to the disappearance of local minimum when switching from a source position to another; are solved through a weighting process by a Hanning window in time and frequency thus allowing to find the location of an unknown position of the source.

#### ACKNOWLEDGMENT

The Lebanese authors thank the Lebanese University for the financial support of this work.

The authors thank the National Council for Scientific Research (Lebanese CNRS) for the financing of the thesis of Mr Karl Hourany.

#### REFERENCES

- [1] Roux, P., W.A. Kuperman, and t.N. Group, Extracting coherent wave fronts from acoustic ambient noise in the ocean. *The Journal of the Acoustical Society of America*, 2004. 116(4): p. 1995-2003.
- [2] Fried, S.E., et al., Extracting the local Green's function on a horizontal array from ambient ocean noise. *The Journal of the Acoustical Society of America*, 2008. 124(4): p. EL183-EL188.
- [3] Sabra, K.G., P. Roux, and W.A. Kuperman, Arrival-time structure of the time-averaged ambient noise cross-correlation function in an oceanic waveguide. *The Journal of the Acoustical Society of America*, 2005. 117(1): p. 164-174.
- [4] Shapiro, N.M. and M. Campillo, Emergence of broadband Rayleigh waves from correlations of the ambient seismic noise. *Geophysical Research Letters*, 2004. 31(7): p. L07614.
- [5] Sabra, K.G., et al., Surface wave tomography from microseisms in Southern California. *Geophysical Research Letters*, 2005. 32(14): p. L14311.
- [6] Larose, E., et al., Correlation of random wavefields: An interdisciplinary review. *Geophysics*, 2006. 71(4): p. SI11-SI21.
- [7] Moulin, E., et al., Applicability of acoustic noise correlation for structural health monitoring in nondiffuse field conditions. *Applied Physics Letters*, 2009. 95(9): p. 094104.
- [8] Hadzioannou, C., et al., Stability of monitoring weak changes in multiply scattering media with ambient noise correlation: Laboratory experiments. *The Journal of the Acoustical Society of America*, 2009. 125(6): p. 3688-3695.
- [9] Moulin, E., et al., Applicability of acoustic noise correlation for structural health monitoring in nondiffuse field conditions. *Applied Physics Letters*, 2009. 95(9): p. 094104-094104-3.
- [10] Leyla, N.A., et al., Structural Health Monitoring using cross-correlation of an ambient noise field. *The Journal of the Acoustical Society of America*, 2008. 123(5): p. 3698-3698.
- [11] Leyla, N.A., et al., Parameter study for Structural Health Monitoring based on ambient noise cross-correlation. *The Journal of the Acoustical Society of America*, 2009. 125(4): p. 2635-2635.
- [12] J. B. Allen and D. A. Berkley. Image methode for efficiently simulating small-room acoustics. *J. Acoust. Soc. Am.*, 65 :943-950, 1979. 14, 15
- [13] F. B. Mechel. Improved mirror source method in room acoustics. *Journal of Sound and vibration*, 256 :873-940, 2002. 14
- [14] K. Hourany, F. Benmeddour, E. Moulin, J. Assaad and Y. Zaatari. Calculation of the similarity rate between images based on the local minima present therein. *Lebanese Science Journal*, Vol. 17, No. 2, 2016